Uncertainty quantification for nonlinear waves in liquid crystals using multi-level Monte Carlo

Peder Aursand[a,*], Jonas Šukys[b]

[a] *Department of Mathematical Sciences, Norwegian University of Science and Technology, NO–7491 Trondheim, Norway.*

[b] *Computational Science and Engineering Laboratory, ETH Zürich, CH–8092 Zürich, Switzerland.*

Abstract

We consider a variational wave equation giving the evolution of the director field of a nematic liquid crystal. The nonlinearity of this wave equation is strongly dependent on the material constants describing the elasticity of the system. Using the multi-level Monte Carlo (MLMC) Finite-Volume sampling method we quantify the influence of uncertain material constants and uncertain initial data on the initial-value problem. The MLMC scheme involves sampling solutions of the Stochastic PDE on a hierarchy of nested meshes. We present results from uncertainty quantification on waves in the director field in both 1D and 2D. Herein, we observe that 5-10 times the computational work is required to achieve a desired accuracy in the estimated mean when using a standard Monte Carlo method compared to when using the MLMC scheme.

Keywords: Uncertainty quantification, Nematic liquid crystals, Nonlinear waves, Multi-level Monte Carlo

1. Introduction

The term liquid crystal refers to a state of matter with both crystalline characteristics as well as properties normally associated with liquids. For specific materials, the liquid crystal phase can be observed in certain ranges of temperature, mixture concentrations, or both. Nematic liquid crystals usually consists of elongated molecules for which it is energetically favorable for neighboring molecules to align. Therefore, even though the molecules are free to flow, one can observe macroscopic correlation of the orientation of their long axis. Since the refractive index of the material depends on the molecular orientation, and since the orientation can be influenced by external electromagnetic fields, nematic liquid crystals have seen widespread use in display devices.

Under the assumption of constant local degree of orientation, the state of a nematic liquid crystal is traditionally represented in terms of two linearly independent vector fields:

*Corresponding author

Email addresses: peder.aursand@math.ntnu.no (Peder Aursand), jonas.sukys@math.ethz.ch (Jonas Šukys)

the velocity field and the director field. The latter is a map

$$\mathbf{n} : \mathbb{R}^3 \times [0, \infty) \to \mathbb{S}^2$$

from Euclidean space to the unit ball. In the present work we assume a stationary flow field and will focus on the dynamics of the director field.

The dynamics of the director field can be derived using an energy variational approach. Herein, the elastic energy density associated with distortion of the director field is given by the Oseen–Franck functional

$$\mathbf{W}(\mathbf{n}, \nabla\mathbf{n}) = \alpha \left|\mathbf{n} \times (\nabla \times \mathbf{n})\right|^2 + \beta \left(\nabla \cdot \mathbf{n}\right)^2 + \gamma \left(\mathbf{n} \cdot (\nabla \times \mathbf{n})\right)^2. \tag{1.1}$$

It can be shown that (1.1) is the general form of an energy that is quadratic in $\nabla\mathbf{n}$ and invariant under the transformation $\mathbf{n} \to -\mathbf{n}$ [5]. The constants α, β and γ are material constants of the liquid crystal, and are associated with the three basic types of deformations of the medium; bend, splay and twist; respectively. Assuming zero dissipation, the evolution of the director $\mathbf{n}$ is then given by the principle of least action

$$\delta \iint \left(\mathbf{n}_t^2 - \mathbf{W}(\mathbf{n}, \nabla\mathbf{n})\right) \, \mathrm{d}x \, \mathrm{d}t = 0, \qquad \mathbf{n} \cdot \mathbf{n} = 1. \tag{1.2}$$

Standard calculations reveal that the *Euler-Lagrange* equation associated with (1.2) is the *variational wave equation*

$$\mathbf{n}_{tt} = \frac{\operatorname{div}\left(\mathbf{W}_{\nabla\mathbf{n}}(\mathbf{n}, \nabla\mathbf{n})\right) - \mathbf{W}_{\mathbf{n}}(\mathbf{n}, \nabla\mathbf{n})}{2}.$$

A simple one-dimensional model can be derived by assuming that the director field depends on a single space variable x, and, that the director field $\mathbf{n}$ in confined to the x-y plane. The director can then be written as

$$\mathbf{n} = (\cos u(x,t),\, \sin u(x,t),\, 0).$$

Here, u denotes the angle between the long axis of the molecules and the x-axis. The variational wave equation describing the dynamics of planar waves in 1D is then given by

$$u_{tt} - c(u)\left(c(u)u_x\right)_x = 0, \tag{1.3}$$

where

$$c(u) = \sqrt{\alpha \cos^2(u) + \beta \sin^2(u)}$$

is the nonlinear wave speed. The equation (1.3) was first introduced by Saxton [22], and has since been subject the numerous studies due to its interesting nonlinear properties [13, 9, 12]. Recently, there has also been some effort towards making efficient, stable and convergent numerical schemes for the initial-value problem [11, 15].

A similar model can be derived in 2D by asserting

$$\mathbf{n} = (\cos u(x,y,t),\, \sin u(x,y,t),\, 0)\,.$$

In this case, the variational wave equation takes the form

$$u_{tt} - (T(u)\nabla) \cdot (T(u)\nabla u) = 0 \tag{1.4}$$

with

$$T(u) = \begin{pmatrix} \sqrt{\alpha}\cos(u) & \sqrt{\alpha}\sin(u) \\ \sqrt{\beta}\sin(u) & -\sqrt{\beta}\cos(u) \end{pmatrix}.$$

The material constants α and β play a crucial role in the nonlinear dynamics of the planar waves described by (1.3) and (1.4). In the modeling of nematic liquid crystals, the value of these can be subject to uncertainties based on e.g. errors bars in their experimental measurement and simplifications in their dependence on temperature [6]. Moreover, one might wish to study the dynamics of the director field over a range of temperatures. To this end, the problems (1.3) and (1.4) can be recast as the stochastic initial-value problems

$$u_{tt} - c(u,\omega)\left(c(u,\omega)u_x\right)_x = 0, \qquad (x,t) \in \mathbb{R} \times [0,T], \tag{1.5a}$$
$$u(x,0) = u_0(x,\omega), \qquad x \in \mathbb{R}, \tag{1.5b}$$
$$u_t(x,0) = u_1(x,\omega), \qquad x \in \mathbb{R}, \tag{1.5c}$$

and

$$u_{tt} - (T(u,\omega)\nabla) \cdot (T(u,\omega)\nabla u) = 0, \qquad (x,y,t) \in \mathbb{R}^2 \times [0,T], \tag{1.6a}$$
$$u(x,y,0) = u_0(x,y,\omega), \qquad (x,y) \in \mathbb{R}^2, \tag{1.6b}$$
$$u_t(x,y,0) = u_1(x,y,\omega), \qquad (x,y) \in \mathbb{R}^2, \tag{1.6c}$$

where $\omega \in \Omega$, for some probability space $(\Omega, \mathcal{F})$.

Uncertainty quantification for solutions of partial differential equations has been an active field of research in recent years [24, 4, 17, 21]. In practical modeling, the physical parameters, initial data, and boundary conditions are often all subject to uncertainty. How to efficiently determine the effect this has on the solutions of nonlinear initial-value problems is a nontrivial issue of great interest in applied sciences and engineering. This is especially true for hyperbolic partial differential equations where solutions might develop shocks and discontinuities [24, 21].

An important class of methods for uncertainty quantification for PDEs is the so-called *non-intrusive* methodology [2]. The main benefit of these types of schemes is that existing code for solving the deterministic problem can be used with few or no changes. Herein, the Monte Carlo sampling method is one of the most notable examples. It relies on sampling the underlying probability space for the initial-value problem, and in each instance solving the deterministic PDE. The ensemble of solutions can then be used to estimate statistical quantities such as the mean and variance.

While non-intrusive and simple to implement, the Monte Carlo sampling method suffers from a low rate of convergence [18]. This issue can be detrimental to performance, especially for uncertainty quantification for PDEs in high spatial dimensions. Here, obtaining even

a single deterministic solution can be computationally expensive. Several techniques have been proposed to assuage the performance issue of Monte Carlo methods. Examples include variance reduction [8] and quasi Monte Carlo methods [7]. In this work we will focus on the *multi-level* Monte Carlo method, first introduced by Heinrich [10] for numerical quadrature. It has since then been successfully applied to hyperbolic conservation laws in conjunction with finite-volume methods [18, 19, 20]. The method relies on performing Monte Carlo sampling on a hierarchy of nested computational grids. By drawing more samples from realizations on coarser grids, where solving the PDE numerically is cheaper, one can efficiently estimate the statistics of the problem.

The asymptotic efficiency of the MLMC method has been rigorously proven for scalar conservation laws, and its performance demonstrated for systems of conservation laws [2]. The potential applicability of this scheme for uncertainty quantification for other nonlinear models in the applied sciences is therefore of great interest. The main purpose of this work is to perform uncertainty quantification for nonlinear waves in liquid crystals in 1D (1.5) and 2D (1.6), using both the MC and MLMC methods. By doing this, we will demonstrate that significant gains in efficiency can be obtained by using MLMC for these variational wave equations. This has, to the best of the authors' knowledge, so far not been the subject of much study.

The paper is organized as follows: Section 2 concerns the deterministic solution of the variational wave equation in 1D and in 2D. Herein, we derive a simple finite-difference scheme that by design preserves the energy stability of the model. In Section 3 we outline how the MC and MLMC methods can used in conjunction with the deterministic solver to perform uncertainty quantification. Section 4 and 5 contains the numerical experiments for 1D and 2D planer waves, respectively. Here, we perform uncertainty quantification using both the basic MC method and the MLMC scheme, and compare their error and efficiency.

2. A Hamiltonian finite-difference method

In order to give a deterministic solution of the initial-value problems (1.5) and (1.6), we employ a finite difference scheme based on the Hamiltonian formulation

$$u_{tt} = -\frac{\delta H}{\delta u}. \tag{2.1}$$

This gives an efficient and robust numerical method that, on the semi-discrete level, respects the underlying energy stability of the model. For time integration we will employ the Leapfrog method.

2.1. The 1D model

In the 1D case (1.3), we have

$$\frac{\delta H}{\delta u} = -c(u)\left(c(u)u_x\right)_x = c(u)c'(u)u_x^2 - \left(c^2(u)u_x\right)_x. \tag{2.2}$$

For a spatial computational domain $[x_0, x_N]$ we denote $x_i = x_0 + i\Delta x$ for $i \in \{0, \cdots, N\}$. Any grid function $u(x,t)$ can then be written $u_i(t) = u(x_i, t)$. Further, by defining the central difference operator as

$$D_0 u_i := \frac{u_{i+1} - u_{i-1}}{2\Delta x}, \tag{2.3}$$

we can write down the semi-discrete numerical scheme

$$(u_i)_{tt} = c(u_i)c'(u_i)\left(D_0 u_i\right)^2 - D_0\left(c^2(u_i) D_0 u_i\right). \tag{2.4}$$

It is straightforward to show that this scheme preserves a discrete version of the energy [15]. Specifically, at the semi-discrete level, we have

$$\frac{\mathrm{d}}{\mathrm{d}t}\left(\frac{\Delta x}{2}\sum_{i=0}^{N}\left((u_i)_t^2 + c^2(u_i)\left(D_0 u_i\right)^2\right)\right) = 0 \tag{2.5}$$

given periodic boundary conditions or decaying data.

2.2. The 2D model

For the 2D equation (1.4), we have,

$$\begin{aligned}\frac{\delta H}{\delta u} &= c(u)c'(u)u_x^2 - \left(c^2(u)u_x\right)_x + b(u)b'(u)u_y^2 - \left(b^2(u)u_y\right)_y + a'(u)u_x u_y - (a(u)u_y)_x - (a(u)u_x)_y \\ &= -c^2(u)u_{xx} - c(u)c'(u)u_x^2 - b^2(u)u_{yy} - b(u)b'(u)u_y^2 - a'(u)u_x u_y - 2a(u)u_{xy} \\ &= -c(u)\left(c(u)u_x\right)_x - b(u)\left(b(u)u_y\right)_y - a'(u)u_x u_y - 2a(u)u_{xy}.\end{aligned}$$

Similarly as before, we can for a computational domain $[x_0, x_N] \times [y_0, y_N]$ denote $u_{ij}(t) = u(x_i, y_j, t)$, where $x_i = x_0 + i\Delta x$ and $y_j = y_0 + j\Delta y$. Again, we define central difference operators

$$D_0^x u_{ij} := \frac{u_{i+1,j} - u_{i-1,j}}{2\Delta x} \text{ and } D_0^y u_{ij} = \frac{u_{i,j+1} - u_{i,j-1}}{2\Delta y}. \tag{2.6}$$

This allows us to write down the semi-discrete finite-difference scheme

$$\begin{aligned}(u_{ij})_{tt} + c(u_{ij})c'(u_{ij})(D_0^x u_{ij})^2 - D_0^x\left(c^2(u_{ij})D_0^x u_{ij}\right) + b(u_{ij})b'(u_{ij})(D_0^y u_{ij})^2 - D_0^y\left(b^2(u_{ij})D^y u_{ij}\right) \\ + a'(u_{ij})D_0^x(u_{ij})D_0^y(u_{ij}) - D_0^x\left(a(u_{ij})D_0^y u_{ij}\right) - D_0^y\left(a(u_{ij})D_0^x u_{ij}\right) = 0.\end{aligned} \tag{2.7}$$

Note that in the above we have assumed that the grid parameter N is the same in the x and y dimensions. This is a simplification made for the purpose of this exhibition, and not a limitation inherent to the scheme.

The scheme (2.7) can be shown to preserve a discrete version of the energy of the model [1]. Specifically, solutions fulfill

$$\frac{d}{dt}\left(\frac{\Delta x \Delta y}{2}\sum_{i,j}(u_{ij})_t^2 + c^2(u_{ij})\left(D_0^x u_{ij}\right)^2 + b^2(u_{ij})\left(D_0^y u_{ij}\right)^2 + 2a(u_{ij})D_0^x(u_{ij})D_0^y(u_{ij})\right) = 0$$

given periodic boundary conditions or decaying data.

3. Uncertainty quantification using multi-level Monte Carlo

Given a stable and efficient numerical scheme for solving the deterministic initial value problems (1.3) and (1.4), a Monte Carlo (MC) type scheme can be applied to perform uncertainty quantification (for instance, to estimate the mean value and the variance of the solution u) for the stochastic initial-value problems (1.5) and (1.6).

3.1. The Monte Carlo Finite-Volume method

The Monte Carlo Finite-Volume sampling method can be summed up to three basic steps:

1. Draw M independent identically distributed samples of α^k, β^k, u_0^k and u_1^k for $k = 1, \ldots, M$.

2. For each realization $\{\alpha^k, \beta^k, u_0^k, u_1^k\}$ we solve the initial-value problem using the deterministic numerical method with a fixed mesh. The numerical solutions are denoted by u^k, $k = 1, \ldots, M$.

3. Estimate the expectation of the random solution field by calculating the sample mean

$$E_M[u] := \frac{1}{M} \sum_{k=1}^{M} u^k. \tag{3.1}$$

Higher statistical moments such as the variance can also be estimated [23].

Different strategies exist for choosing the number of samples M for a given mesh number N [23]. In this work we will use $M = N$ for all MC calculations.

3.2. The multi-level Monte Carlo Finite-Volume method

The deterministic solution of the initial value problem can be expensive, especially in higher dimensions. Indeed, calculating a large number of samples using a very fine mesh can in many cases be computationally infeasible. The *multi-level* Monte Carlo Finite-Volume (MLMC) method is one way of assuaging this concern. It relies on taking Monte Carlo samples on a hierarchy of nested grids. By taking more samples on the coarser grid, where the numerical approximation of the deterministic problem is computationally cheaper, one can obtain the same order of accuracy at a significantly lower cost compared to the MC method.

In this work we use Cartesian grids, and for the level $\ell \in \{0, \cdots, L\}$ we denote

$$\Delta x_\ell = 2^{-\ell} \Delta x_0,$$

for some fixed coarsest mesh size Δx_0. For simplicity, we assume equal spatial mesh sizes in both dimensions for the 2D model. The MLMC method consists of the three main steps:

1. For each level $\ell \in \{0, \ldots, L\}$, draw a level-dependent number M_ℓ independent identically distributed samples α_ℓ^k, β_ℓ^k, $u_{0,\ell}^k$ and $u_{1,\ell}^k$ for $k = 1, \ldots, M_\ell$.

2. For each realization $\{\alpha_\ell^k, \beta_\ell^k, u_{0,\ell}^k, u_{1,\ell}^k\}$ of the parameters solve the deterministic initial value problem. The numerical solutions are denoted by u_ℓ^k, $k = 1, \ldots, M_\ell$.

3. Estimate the expectation of the random solution field by using the estimator

$$E^L[u] := E_{M_0}[u_0] + \sum_{\ell=0}^{L} E_{M_\ell}[u_\ell - u_{\ell-1}], \tag{3.2}$$

where $E_M[u]$ denotes the MC estimator (3.1). Higher statistical moments can be calculated in a similar manner [23].

There are different strategies for choosing the level-dependent number of samples M_ℓ. In this work we will use

$$M_\ell = M_L 2^{2(L-\ell)},$$

a choice designed to equilibrate the error contributions from each successive level, given a first-order deterministic solver [23]. Note, however, that rigorous error estimates for MLMC only exist for scalar conservation laws [16].

For the reader's reference, we emphasize that the MLMC estimates in the rest of this paper are all determined by the following list of parameters:

M_L	Number of samples on the finest mesh level
N_L	Number of cells in each direction in finest mesh
L	Number of levels of refinement

3.3. Computation of sample statistics

When the number of samples is large, storage saving techniques should be used when assembling statistical estimates. For efficient and stable computation of the mean and variance we employ the following on-line algorithm due to Knuth [14]: Let $\bar{u}^0 = 0$ and $\Phi^0 = 0$. Given samples $u^i, i \in \{1, \ldots, M\}$ we can proceed iteratively to calculate

$$\bar{u}^i = \sum_{j=1}^{i} \frac{u^j - \bar{u}^{j-1}}{i}, \qquad \Phi^i = \Phi^{i-1} + \left(u^j - \bar{u}^{j-1}\right)\left(u^j - \bar{u}^j\right).$$

Unbiased estimates for the mean and variance of the population are then given by

$$E_M[u] = \bar{u}^M \qquad \text{and} \qquad \mathrm{Var}_M[u] = \frac{\Phi^M}{M-1},$$

respectively. This allows us to update the statistical estimates after calculating each individual samples, eliminating the need for storing all solutions and thereby significantly reducing memory requirements.

Since individual samples only interact when combining the statistical estimates, the MC and MLMC methods are both highly parallelizable. In practice, a parallel implementation will require us to be able to combine statistical estimates from smaller subsets of samples.

To this end, the following algorithm proposed by Chan et al. [3] can be used: Let $E_{M_A}[u]$ and $E_{M_B}[u]$ be estimates for the mean for sample sizes M_A and M_B, respectively, with $M = M_A + M_B$. The combined mean can then be calculated as

$$E_M[u] = \frac{M_A E_{M_A}[u] + M_B E_{M_B}[u]}{M}$$

and for the variance

$$\Phi_M[u] = \Phi_{M_A}[u] + \Phi_{M_B}[u] + \frac{M_A M_B}{M} \left(E_{M_A}[u] - E_{M_B}[u]\right)^2,$$

with

$$\mathrm{Var}_M[u] = \frac{\Phi_M[u]}{M-1}.$$

3.4. L^2 stability for the MC mean estimator

The equation (1.3) can be derived from an energy law. Hence, it inherits an L^2-stability from the underlying energy functional. It is straightforward to verify that smooth solutions $u(x,t)$ of (1.3) satisfy

$$\frac{\mathrm{d}}{\mathrm{d}t}\mathcal{E}_u(t) = \frac{\mathrm{d}}{\mathrm{d}t}\int \left(u_t^2 + c^2(u)u_x^2\right) \mathrm{d}x = 0.$$

For positive (and nonzero) α and β this implies

$$\int \left(u_t^2 + \min\{\alpha,\beta\}u_x^2\right) \mathrm{d}x \le \mathcal{E}_u(t) \le \int \left(u_t^2 + \max\{\alpha,\beta\}u_x^2\right) \mathrm{d}x \tag{3.3}$$

giving a basic stability estimate. In Section 2 we showed that this energy principle is shared by the deterministic solvers at the semi-discrete level.

We can verify that this stability also holds for the MC mean estimator as follows: Assume that u and v are two smooth solutions of (1.3), thus satisfying (3.3). For the mean $w = (1/2)(u+v)$ we then have

$$\begin{aligned}
\mathcal{E}_w(t) = \int \left(w_t^2 + c^2(w)w_x^2\right) \mathrm{d}x &= \frac{1}{4}\int \left(u_t^2 + c^2(w)u_x^2\right) \mathrm{d}x + \frac{1}{4}\int \left(v_t^2 + c^2(w)v_x^2\right) \mathrm{d}x \\
&\quad + \frac{1}{2}\int \left(v_t u_t + c^2(w)u_x v_x\right) \mathrm{d}x \\
&\le \frac{1}{4}\int \left(u_t^2 + \max\{\alpha,\beta\}u_x^2\right) \mathrm{d}x + \frac{1}{4}\int \left(v_t^2 + \max\{\alpha,\beta\}v_x^2\right) \mathrm{d}x \\
&\quad + \frac{1}{2}\int \left(|v_t u_t| + \max\{\alpha,\beta\}|u_x v_x|\right) \mathrm{d}x \\
&\le \frac{1}{4}\int \left(u_t^2 + \max\{\alpha,\beta\}u_x^2\right) \mathrm{d}x + \frac{1}{4}\int \left(v_t^2 + \max\{\alpha,\beta\}v_x^2\right) \mathrm{d}x \\
&\quad + \frac{1}{4}\int \left(u_t^2 + v_t^2 + \max\{\alpha,\beta\}(u_x^2 + v_x^2)\right) \mathrm{d}x \\
&= \frac{1}{2}\int \left(u_t^2 + \max\{\alpha,\beta\}u_x^2\right) \mathrm{d}x + \frac{1}{2}\int \left(v_t^2 + \max\{\alpha,\beta\}v_x^2\right) \mathrm{d}x.
\end{aligned} \tag{3.4}$$

That the same holds for the MC mean estimator (3.1), i.e.

$$\mathcal{E}_{E_M[u]}(t) \leq \frac{1}{M} \sum_{k=1}^{M} \int \left(\left(u_t^k\right)^2 + \max\{\alpha, \beta\} \left(u_x^k\right)^2 \right) \mathrm{d}x,$$

follows by induction.

An analogous result for the 2D equation can be obtained in an analogous way.

4. 1D planar waves

In the following, we investigate the propagation of nonlinear 1D planar waves with uncertain, uniformly distributed elastic constants. Specifically, we let the material constants be independent identically distributed variables with

$$\alpha \sim \mathcal{U}(0.3, 0.7), \qquad \beta \sim \mathcal{U}(1.3, 1.7), \tag{4.1}$$

and study the initial value problem (1.5) with

$$u_0(x) = \frac{\pi}{4} + \exp(-x^2) \tag{4.2a}$$

$$u_1(x, \omega) = -c(u_0, \omega) u_{0,x}(x). \tag{4.2b}$$

Notice that this introduces uncertainty in both the flux term as well as in the initial data.

Figure 4.1 shows the estimated mean and standard deviation of the director field using the MC method with $M = N = 512$. Figure 4.2 shows the same estimates, but using the

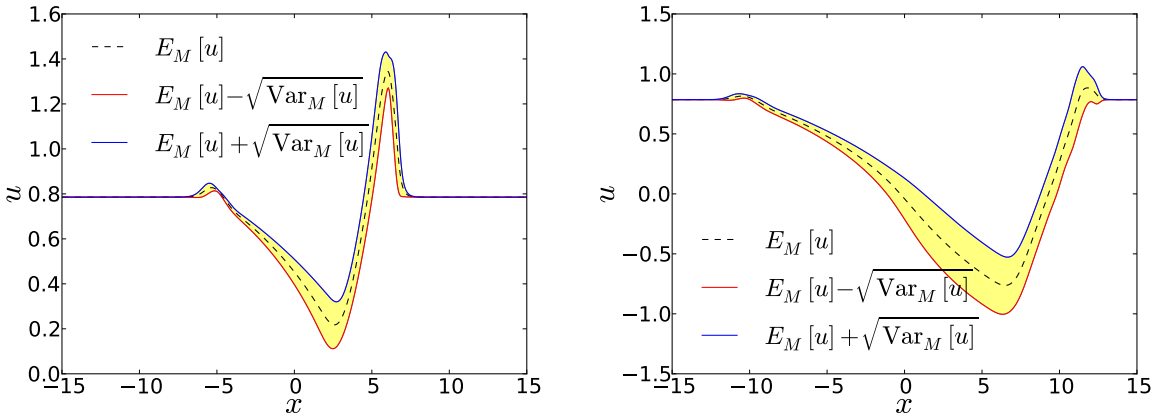

(a) $t = 5$ (b) $t = 10$

Figure 4.1: The mean and standard deviation of the director field for the initial value problem (4.2) with α and β given by (4.1). Calculated using the MC method with $M = N = 512$.

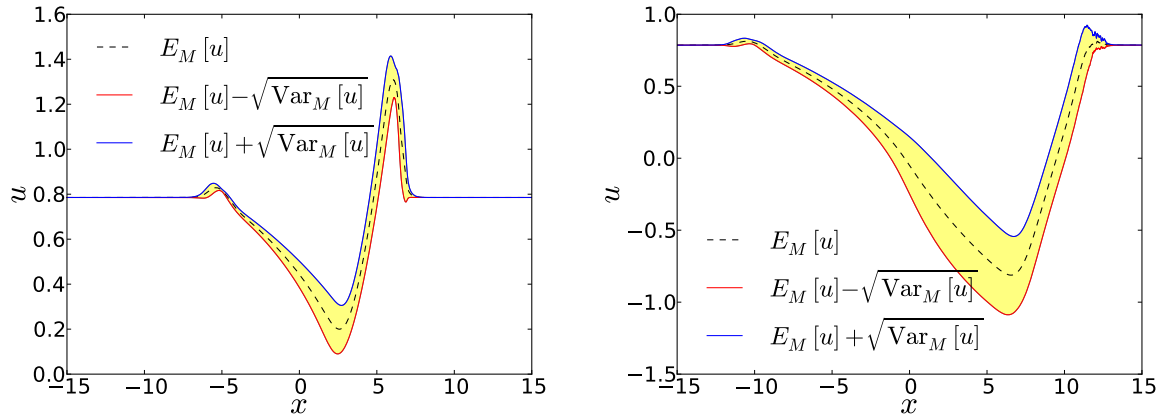

(a) $t = 5$ (b) $t = 10$

Figure 4.2: The mean and variance of the director field for the initial value problem (4.2) with α and β given by (4.1). Calculated using the MLMC method with $M_L = 64$, $L = 7$ and $N_L = 8192$.

MLMC method with $M_L = 64$, $L = 7$ and $N_L = 8192$. From the results, it is clear that the uncertainty in the elastic constants introduce uncertainties in both the magnitude and position of the propagating disturbance. The error bars for the director field, shown in the filled yellow area, are of the order of $\sim 10\%$.

The MLMC estimates, the variance in particular, are more irregular than their MC counterparts, as can be seen in Figure 4.2. This is not unexpected in regions where the solution may vary greatly between levels of mesh refinement, e.g. near shocks and discontinuities.

4.1. Convergence and efficiency

We estimate the order of convergence of the MC and MLMC methods for the initial value problem (4.2).

Since the MC and MLMC estimators are themselves random, the root mean square error estimator is employed to extract statistical convergence rates from the fluctuating error measurements. Let $E_{\mathrm{ref}}[u]$ be an accurate reference solution, calculated using the MLMC scheme with a high accuracy. To estimate the error of an MC or MLMC estimator $E_M[u]$ we calculate a sequence of estimates

$$E_M^{(k)}[u], \quad k = 1, \cdots, K$$

for some number K. We then define the root-mean-square relative error as

$$\mathcal{E} = \sqrt{\frac{1}{K}\sum_k^K \left(\mathcal{E}_M^{(k)}\right)^2}, \tag{4.3}$$

where

$$\mathcal{E}_M^{(k)} = \frac{\|E_{\text{ref}}[u] - E_M^{(k)}[u]\|_{L^2}}{\|E_{\text{ref}}[u]\|_{L^2}}.$$

Figure 4.3 shows the error in the mean and the standard deviation for both the MC and MLMC schemes using $K = 20$. For a given mesh refinement N, the MC scheme outperforms the MLMC scheme. This is not unexpected, since the MC estimator is a combination of a large number of samples on the finest grid. However, in terms of computational efficiency, we see a clear advantage of using the MLMC scheme. In fact, the results show that obtaining the same accuracy in the mean using the MC scheme requires approximately 8 times the computational effort. For the standard deviation the gain is not as big, but the MLMC scheme is also more efficient in this case.

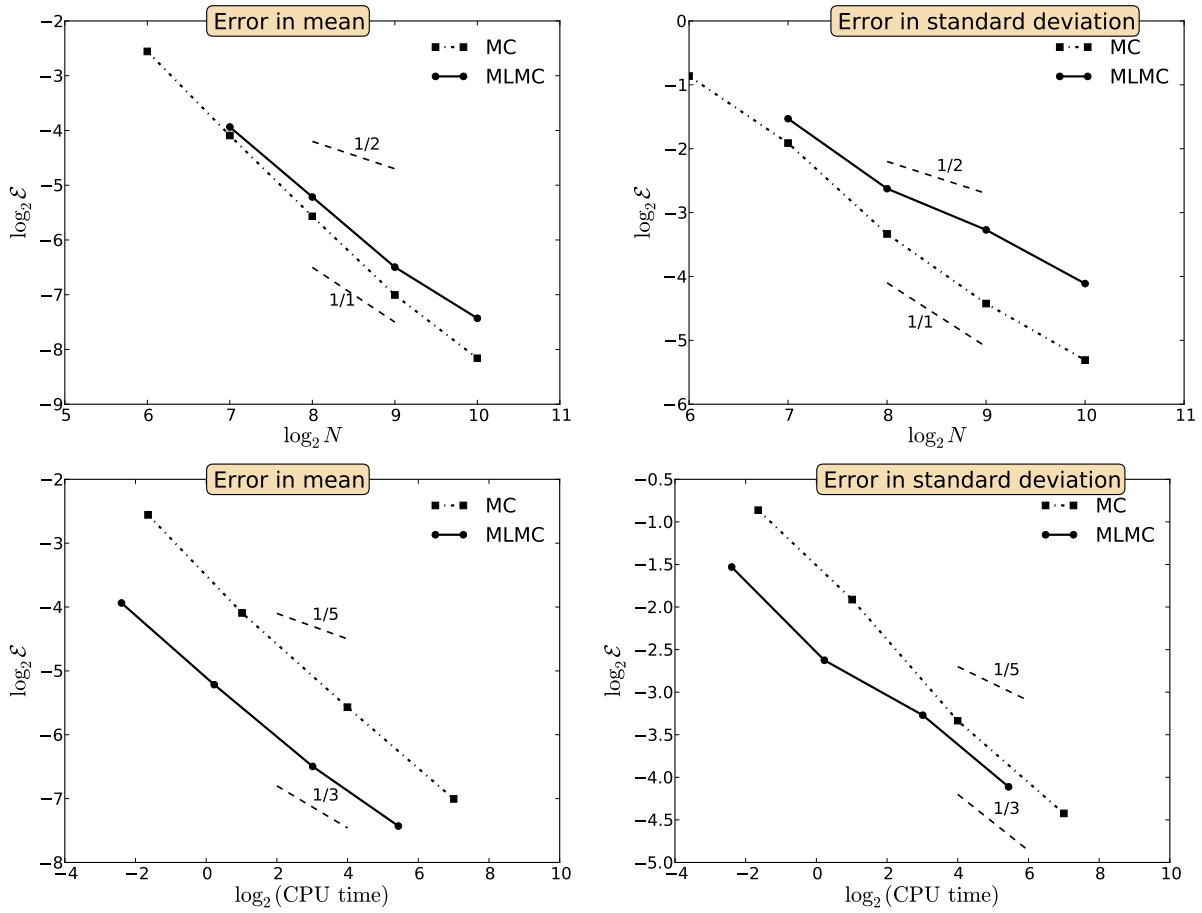

Figure 4.3: Error of the mean and standard deviation for the MC and MLMC method for the initial value problem (4.2) at $t = 5$. The reference solution was calculated using $M_L = 64$, $N_L = 8196$ and $L = 7$. The error ε was calculated using the estimator (4.3) with $K = 20$. Dashed lines indicate expected orders of convergence for scalar conservation laws.

5. 2D planar waves

In what follows, we investigate the evolution of the 2D variational wave equation given uncertain elastic constants α and β. For the deterministic numerical solution of the initial value problem (1.6) we use the Hamiltonian scheme described in Section 2.2.

5.1. Gaussian disturbance

We consider the following initial data, representing a Gaussian disturbance to an initially homogeneous initial state:

$$u_0(x, y) = \exp\left(-\left(x^2 + y^2\right)\right) \tag{5.1a}$$

$$u_1(x, y, \omega) = -c(u_0, \omega)u_{0,x}(x, y) \tag{5.1b}$$

Furthermore, we let the elastic constants be independent identically distributed random variables given by

$$\alpha \sim \mathcal{U}(0.3, 0.7) \qquad \text{and} \qquad \beta \sim \mathcal{U}(1.3, 1.7). \tag{5.2}$$

Note that this introduces uncertainty in both the governing equation as well as in the initial data.

Figure 5.1 shows the mean and the standard deviation of the director angle and its gradient at $t = 10$, calculated using the Monte Carlo method with $M = N = 512$. Similarly,

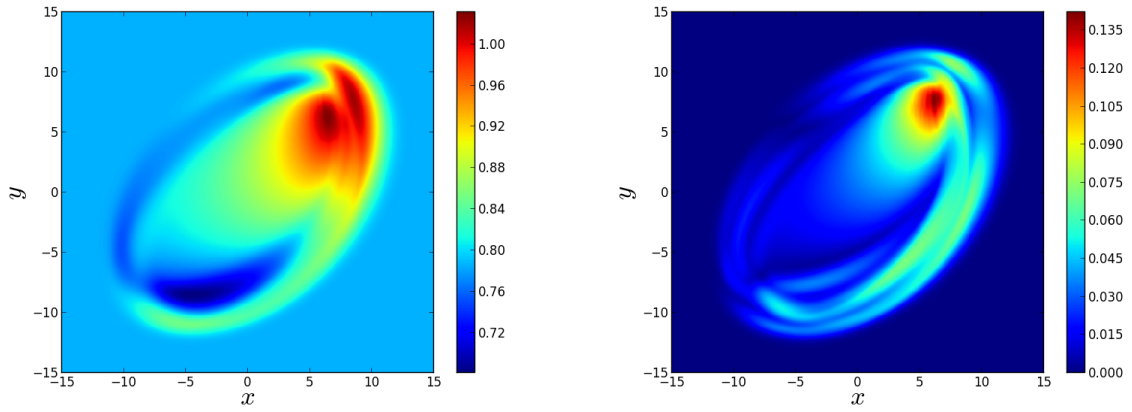

(a) Mean (b) Standard deviation

Figure 5.1: The mean and standard deviation of the director field u at $t = 10$ for the initial value problem (5.1). Calculated using the MC method with $M = N = 512$.

Figure 5.2 shows the mean and the standard deviation calculated using the MLMC scheme with 6 levels ($L = 5$), $M_L = 8$ samples on the fines level with 2048×2048 grid cells. The results illustrate the effect of the nonlinearity. There is a clear preferred direction of propagation, and herein a steepening of the slope can be observed. We also observe that the uncertainty is greatest closest to this propagation front, and the relative standard deviation here is about $\sim 10\%$.

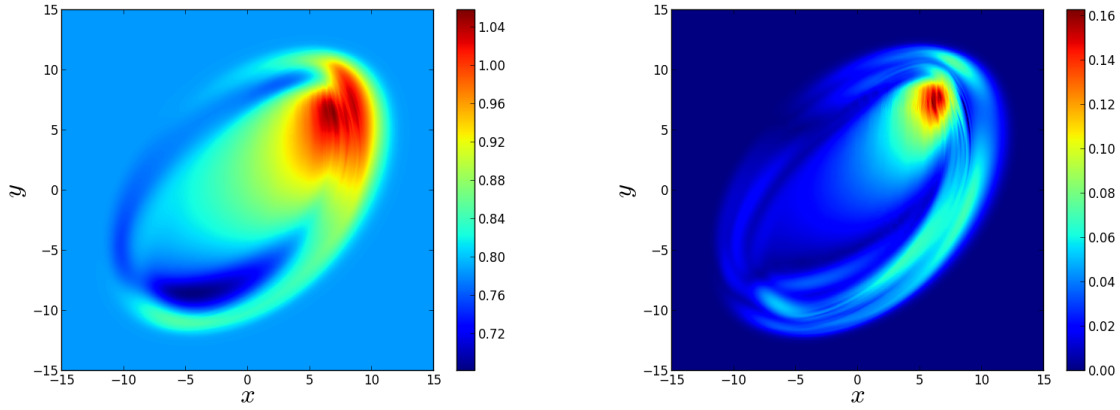

(a) Mean (b) Standard deviation

Figure 5.2: The mean and standard deviation of the director field u at $t = 10$ for the initial value problem (5.1). Calculated using the MLMC method with $M_L = 8$, $L = 5$ and $N_L = 2048$.

5.2. Convergence and efficiency

We study the convergence of the MC and MLMC methods using the initial value problem (5.1). As a reference we use the solution displayed in Figure 5.2. Similarly as before, we use a root-mean-square estimate (4.3) for the error.

Figure 5.3 shows the error (4.3) for both the MC and MLMC schemes using $K = 20$. For a fixed grid accuracy N the MC scheme outperforms the MLMC scheme, which is not unexpected. However, as in the 1D case, the efficiency of the MLMC scheme (error per CPU second) is far superior. In fact, obtaining a lower error in the mean with the MC method requires more than five times the computational efforts. For the standard deviation the difference is not as obvious, but also here the MLMC scheme is superior in terms of efficiency.

5.3. Relaxation from standing wave

A second test case is given by the initial data

$$u_0(x, y) = 2\cos(2\pi x)\sin(2\pi x) \tag{5.3a}$$
$$u_1(x, y) = \sin(2\pi(x - y)) \tag{5.3b}$$

on $(x, y) \in [0, 1] \times [0, 1]$ with periodic boundary conditions. Initially, the director field is a standing wave, something that can be caused by the influence of e.g. an electric field or mechanical vibrations. At $t = 0$ the external influence is switched off, and the dynamics of the director field is governed by the elasticity of the liquid crystal.

We consider the stochastic initial value problem consisting of (1.4) with the initial data (5.3). The elastic constants are assumed to be identically uniformly distributed as

$$\alpha \sim \mathcal{U}(0.45, 0.55) \qquad \text{and} \qquad \beta \sim \mathcal{U}(1.45, 1.55). \tag{5.4}$$

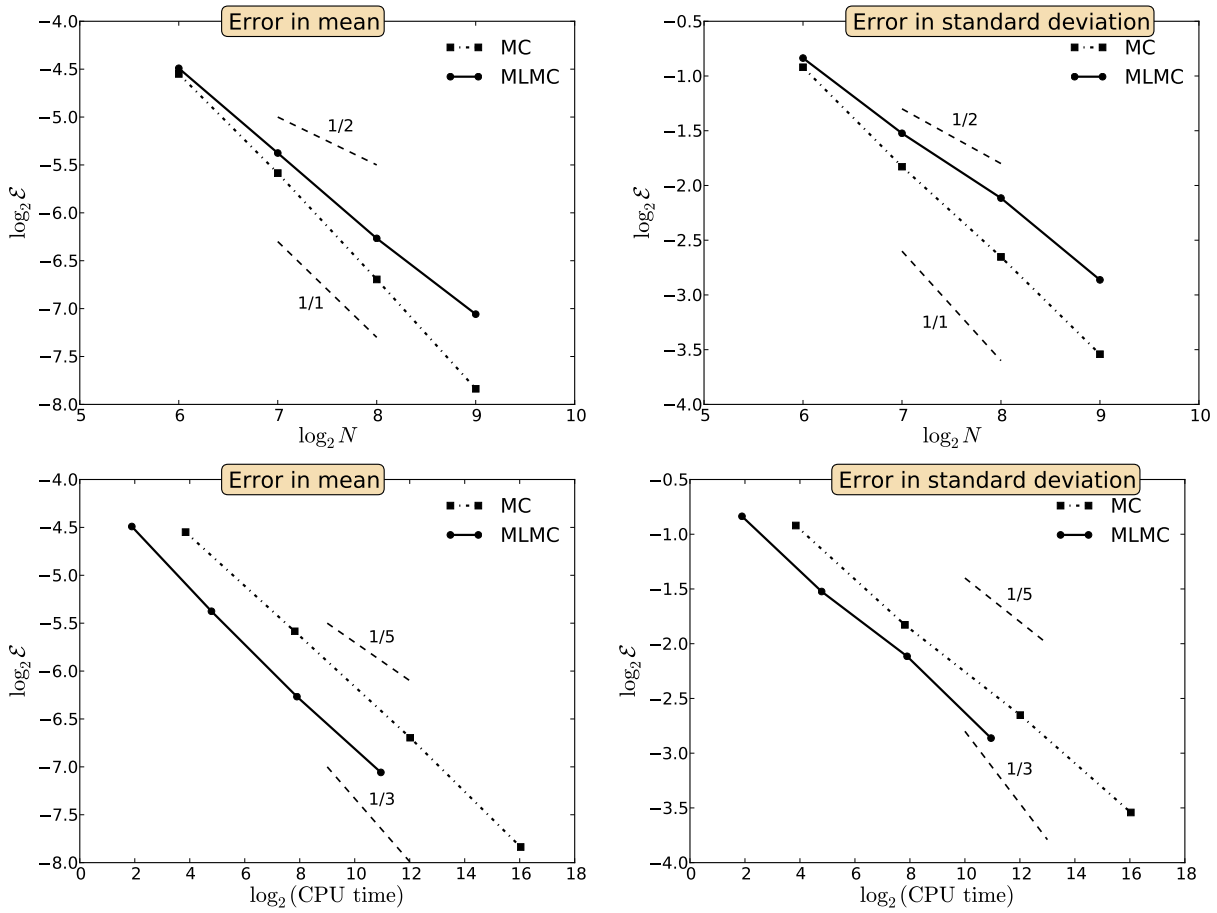

Figure 5.3: Error of the mean and standard deviation of the director field u for the MC and MLMC method for the initial value problem (5.1). The reference solution was calculated using $M_L = 8$, $N_L = 2048$ and $L = 6$. The error ε was calculated using the estimator (4.3) with $K = 20$. Dashed lines indicate expected orders of convergence for scalar conservation laws.

Figure 5.4 shows the estimated mean and standard deviation of the director field at $t = 2$ using the MC method with $M = N = 512$. Similarly, Figure 5.5 shows the estimated

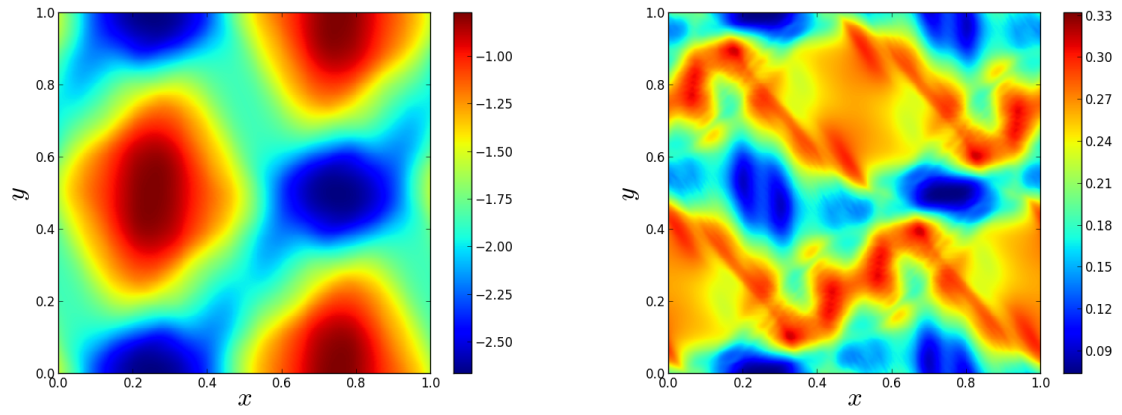

(a) Mean

(b) Standard deviation

Figure 5.4: The mean and standard deviation of the director field u at $t = 2$ for the initial value problem (5.3). Calculated using the MC method with $M = N = 512$.

mean and standard deviation of the director field using the MLMC method with $M_L = 8$, $L = 5$ and $N_L = 2048$. The results show the sinusoidal initial wave deteriorating into a more irregular pattern, while the mean still maintains the same periodicity. The variance is clearly largest between the local maxima, indicating that the elastic constants strongly affect both the position and shape of these.

5.4. Convergence and efficiency

We can study the convergence of the MC and MLMC methods also for this case. Figure 5.6 shows the RMS error (4.3) at $t = 2$ for both the MC and MLMC schemes using $K = 20$. The results read similar as before. In terms of error per grid size the MC method is superior. However, since most of the sampling in the MLMC method is done on coarse grids, the efficiency of this method is much greater. Specifically, Figure 5.6 shows that obtaining the same error in the mean using the MC method requires more than 10 times the computational effort.

6. Summary

We have studied the evolution of a class of nonlinear waves in the director field of nematic liquid crystals with uncertain elastic constants and uncertain initial data. Herein, we perform uncertainty quantification on the stochastic initial-value problem in 1D and 2D using the Monte Carlo and the multi-level Monte Carlo methods. As the deterministic solver we have used a Hamiltonian finite-difference scheme designed to preserve the energy stability inherent to the model.

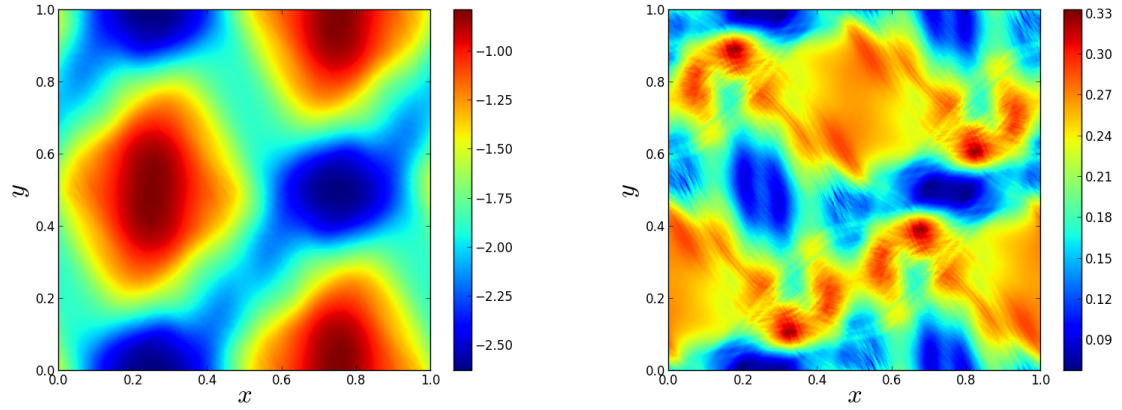

(a) Mean

(b) Standard deviation

Figure 5.5: The mean and standard deviation of the director field u at $t = 2$ for the initial value problem (5.3). Calculated using the MLMC method with $M_L = 8$, $L = 5$ and $N_L = 2048$.

The results, both in 1D and 2D, indicate that the MLMC method can be applied successfully to estimate statistical quantities for models of this kind. In terms of error per computational effort, we observed that the MLMC clearly outperformed the regular MC method. In particular, the results show that in order to obtain the same error in the expectation, the MC method requires 5-10 times the computational work. The efficiency of the MLMC method for the estimation of the variance is lower. However, the obtained numerical results show a clear advantage from using the MLMC scheme also here.

Acknowledgements

The work of Peder Aursand has been funded by the Research Council of Norway project number 213638. The authors are grateful to professor Siddhartha Mishra for his help and advice in the preparation of this manuscript.

References

[1] P Aursand and U. Koley. Higher-order energy stable schemes for a nonlinear variational wave equation modeling nematic liquid crystals in two dimensions. *Preprint*, 2014.

[2] H. Bijl, D. Lucor, S. Mishra, and C. Schwab. *Uncertainty Quantification in Computational Fluid Dynamics*, volume 92. Springer Science & Business Media, 2013.

[3] T. F. Chan, G. H. Golub, and R. J. LeVeque. Updating formulae and a pairwise algorithm for computing sample variances. In *COMPSTAT 1982 5th Symposium held at Toulouse 1982*, pages 30–41. Springer, 1982.

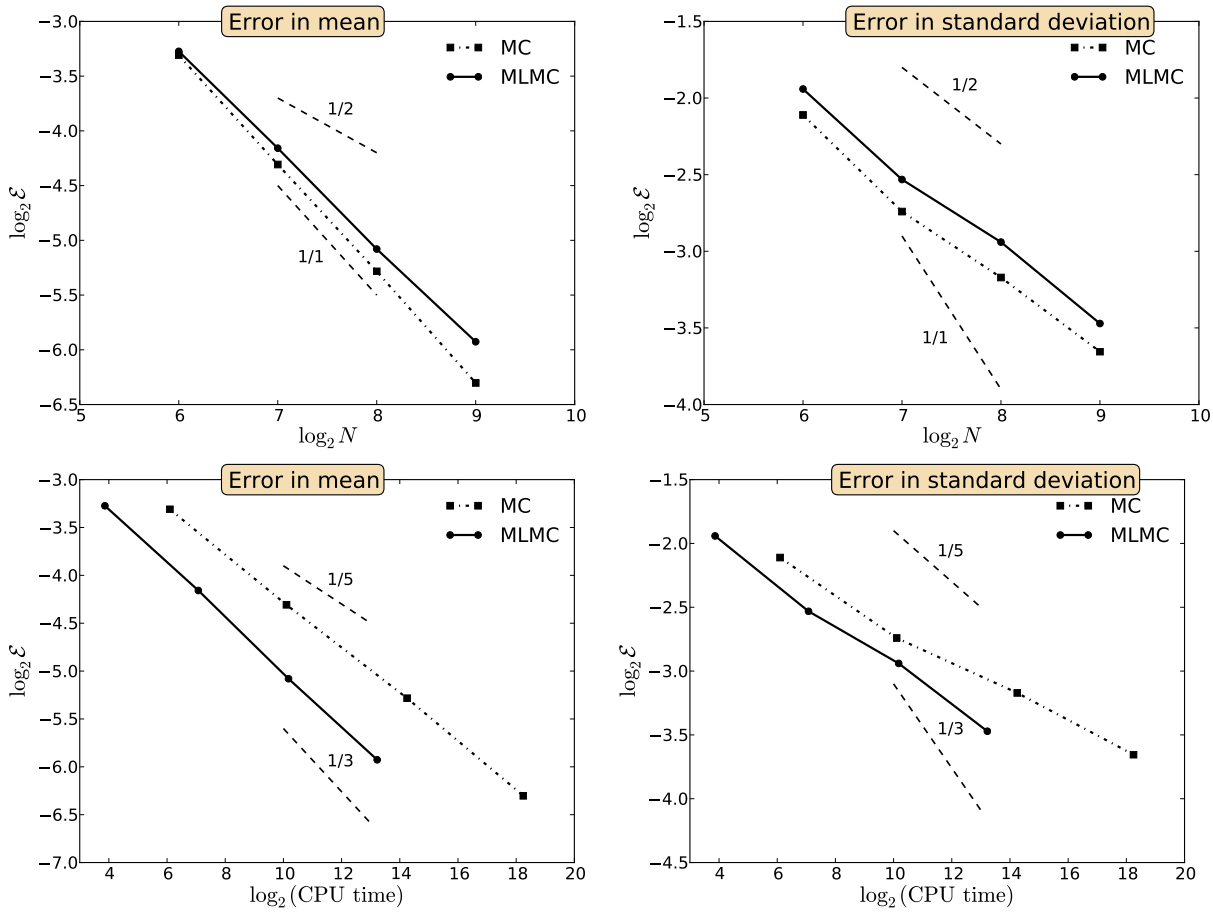

Figure 5.6: Error of the mean and standard deviation of the director field u for the MC method with $M = N$ and the MLMC method with $M_L = 8$ and $L = 4$ for the initial value problem (5.3). The reference solution was calculated using $M_L = 32$, $N_L = 2048$ and $L = 6$. The error ε was calculated using the estimator (4.3) with $K = 20$. Dashed lines indicate expected orders of convergence for scalar conservation laws.

[4] Q.-Y. Chen, D. Gottlieb, and J. S. Hesthaven. Uncertainty analysis for the steady-state flows in a dual throat nozzle. *J. Comput. Phys.*, 204(1):378–398, 2005.

[5] P. G. De Gennes and J. Prost. *The Physics of Liquld Crystals*. Clarendon Press, Oxford, 1993.

[6] W. H. De Jeu, W. A. P. Claassen, and A. M. J. Spruijt. The determination of the elastic constants of nematic liquid crystals. *Mol. Cryst. Liq. Cryst.*, 37(1):269–280, 1976.

[7] J. Dick, F. Y. Kuo, and I. H. Sloan. High-dimensional integration: The quasi Monte-Carlo way. *Acta Numer.*, 22:133–288, 2013.

[8] G. Fishman. *Monte Carlo*. Springer, 1996.

[9] R. T. Glassey, J. K. Hunter, and Y. Zheng. Singularities of a variational wave equation. *J. Diff. Eq.*, 129(1):49–78, 1996.

[10] S. Heinrich. Multilevel monte carlo methods. In *Lecture Notes in Computer Science*, volume 2170 of *Large-scale scientific computing, LSSC 2001, Sozopol, Bulgaria, 2001*, pages 58–67. Springer, 2001.

[11] H. Holden, K. H. Karlsen, and N. H. Risebro. A convergent finite-difference method for a nonlinear variational wave equation. *IMA J. Numer. Anal.*, 29(3):539–572, 2009.

[12] H. Holden and X. Raynaud. Global semigroup of conservative solutions of the nonlinear variational wave equation. *Arch. Rat. Mech. Anal.*, 201(3):871–964, 2011.

[13] J. K. Hunter and R. Saxton. Dynamics of director fields. *SIAM J. Appl. Math.*, 51(6):1498–1521, 1991.

[14] D. Knuth. *The Art of Computer Programming, volume 2: Seminumerical Algorithms*. Addison–Wesley, 1998.

[15] U. Koley, S. Mishra, N. H. Risebro, and F. Weber. Robust finite difference schemes for a nonlinear variational wave equation modeling liquid crystals. *ArXiv e-prints*, 2013.

[16] R. J. LeVeque. *Numerical methods for conservation laws*, volume 132. Springer, 1992.

[17] G Lin, C. H. Su, and G. E. Karniadakis. The stochastic piston problem. *Proceedings of the National Academy of Sciences of the United States of America*, 101(45):15840–15845, 2004.

[18] S. Mishra and C. Schwab. Sparse tensor multi-level Monte Carlo finite volume methods for hyperbolic conservation laws with random initial data. *Math. Comput.*, 81(280):1979–2018, 2012.

[19] S. Mishra, C. Schwab, and J. Šukys. Multi-level Monte Carlo Finite Volume methods for nonlinear systems of conservation laws in multi-dimensions. *J. Comput. Phys.*, 231(8):3365–3388, 2012.

[20] S. Mishra, C. Schwab, and J. Šukys. Multi-level monte carlo finite volume methods for uncertainty quantification of acoustic wave propagation in random heterogeneous layered medium. *Preprint*, 2014.

[21] G. Poëtte, B. Després, and D. Lucor. Uncertainty quantification for systems of conservation laws. *J. Comput. Phys.*, 228(7):2443–2467, 2009.

[22] R. A. Saxton. Dynamic instability of the liquid crystal director. In W. B. Lindquist, editor, *Contemporary Mathematics*, volume 100 of *Current Progress in Hyperbolic Systems, Providence, RI, USA, 1989.*, pages 325–330, 1989.

[23] J. Šukys. *Robust multi-level Monte Carlo Finite Volume methods for systems of hyperbolic conservation laws with random input data*. PhD thesis, Diss., Eidgenössische Technische Hochschule ETH Zürich, Nr. 21990, 2014.

[24] D. Xiu and J. S. Hesthaven. High-order collocation methods for differential equations with random inputs. *SIAM J. Sci. Comput.*, 27(3):1118–1139, 2005.